A model for fluvial channel reaction time during time-dependent climatic and tectonic forcing and its contrary applications

Dr. N.L. Dongre

"The language of light can only be decoded by the heart."

— Suzy Kassem

The Gudra River of Abujhmarh , Bastar,India. :Fluvial incision that predicts the channel topography as a function of time-dependent climatic and tectonic conditions.

Abstract: The fluvial response time dictates the duration of fluvial channel adjustment in response to changing climatic and tectonic conditions. However, when these conditions vary continuously, the channel cannot equilibrate and the response time is not well defined. Here I develop an analytical solution to the linear stream power model of fluvial incision that predicts the channel topography as a function of time-dependent climatic and tectonic conditions. From this solution, a general definition of the fluvial response time emerges: the duration over which the tectonic history needs to be known to evaluate channel topography. This new definition is used in linear inversion schemes for inferring climatic or tectonic histories from river long profiles. The analytic solution further reveals that high-frequency climatic oscillations, such as Milankovitch cycles, are not expected to leave

significant fingerprints on the long profiles of fluvially incised detachment-limited rivers.

---

1 Introduction

The fluvial system responds to changing tectonic and climatic boundary conditions by internally changing the pattern of erosion, sediment transport, and relief. This is mostly understood through a series of coupled interactions acting to bring the fluvial system to a topographic and erosive equilibrium with respect to the external conditions, whereby fluvial incision balances tectonic rock uplift [*Willett and Brandon*, 2002, and references therein].

The question of how fast a fluvial channel responds and changes its characteristics when tectonic or climatic conditions change is of critical importance for assessing the lag time between a change in the boundary conditions, on the one hand, and landscape evolution and sediment flux response, on the other hand [*Godard et al.*, 2013; *Romans et al.*, 2016]. This lag time that controls the probability of finding steady state channels [*Whipple*, 2001], and the prevalence of transient features along fluvial landscapes [*Mudd*, 2016], is commonly referred to as the fluvial response time [*Whipple and Tucker*, 1999; *Allen*, 2008]. The fluvial response time is most easily understood when considering a step change in tectonic or climatic conditions, as the time that it takes for the channel to fully transition from a former to a new steady state topographic [*Whipple*, 2001] or flux [*Willett and Brandon*, 2002; *Armitage et al.*, 2013] conditions. However, when the tectonic and climatic conditions vary continuously, steady state cannot be achieved, and the definition of the response time becomes more elusive.

Estimating the fluvial response time in the field is far from trivial, both because the history of variations of climatic and tectonic conditions is not always known and since identification of steady state conditions in the field is highly speculative [*Willett and Brandon*, 2002]. Numerical investigations of the response time critically depend on the chosen fluvial, climatic, and tectonic parameters [e.g., *Armitage et al.*, 2013; *Godard et al.*, 2013] and cannot always be generalized. These limitations call for an analytical analysis, which can be used to accurately predict rates of landscape evolution and spatial patterns of transiency in response to general histories of the boundary conditions and as a function of the fluvial parameters. To derive an analytical expression, there is a need for a mathematical description of the evolution of fluvial channels as a function of the imposed boundary conditions.

For mountainous bedrock rivers, a description that is widely used in the framework of detachment-limited channels is the stream power model [*Howard and Kerby*, 1983; *Howard*, 1994; *Whipple and Tucker*, 1999]:

$$E = K\, A^m\, S^m \tag{1}$$

where E is the fluvial incision rate ([L/T]), A, is the upstream drainage area ([L^2]), S, is the local slope [L/L], m and n are positive, no integer powers, and K is the erosional efficiency ([$L^{1-2m}T^{-1}$]) that reflects the susceptibility of the landscape to erode. The power law dependency on A and S arises from the postulation that the rate of incision is proportional to the stream power or to the shear stress exerted by the stream on the bed [*Howard and Kerby*, 1983]. This further requires that A acts as a proxy to the water discharge and that K incapsulates climatic conditions, geometrical and hydraulic characteristics of the stream, bedrock resistance to erosion [*Whipple and Tucker*, 1999], and the sediment flux [*Gasparini et al.*, 2007] and its along water column distribution [*Lamb et al.*, 2008]. Several modifications have been suggested to this erosion model,

such as incision thresholds [e.g., *Wilcock*, 1998; *Parker*, 1991; *Snyder et al.*, 2003; *Lague et al.*, 2005; *DiBiase and Whipple*, 2011; *Lague*, 2014], sediment flux-dependent erosion rate [e.g., *Sklar and Dietrich*, 1998; *Lamb et al.*, 2008; *Turowski and Rickenmann*, 2009], and channel width that is sensitive to the rate of tectonic uplift [*Finnegan et al.*, 2005; *Turowski et al.*, 2006; *Amos and Burbank*, 2007; *Attal et al.*, 2008; *Yanites et al.*, 2010]. *Gasparini and Brandon* [2011] have demonstrated that many of these modifications can be accounted for by varying the values of m and n in equation (1), but more important for the current work, the relatively simple form of equation (1) allows developing an analytical solution for the temporal evolution of fluvial channels [e.g., *Royden and Perron*, 2013; *Goren et al.*, 2014].

Using the stream power model to describe fluvial erosion, the evolution of fluvial channels is commonly cast as a topography conservation equation:

$$\frac{\partial z(t,x)}{\partial t} = U(t,x) - K(t,x)A(x)^m \frac{\partial z(t,x)^m}{\partial x}, \quad (2)$$

Where the left-hand side expresses the rate of change of surface elevation, z ([L]), and the right-hand side expresses the balance between the tectonic rock uplift rate or the rate of base level change, U ([L/T]), and the rate of erosion. In equation (2), $S(t,x) = \partial z(t,x)/\partial x$, where x ([L]) is a coordinate system along the channel and t ([T]) is the time. Equation (2) is an advection equation, and therefore, it predicts that perturbations (such as slope break) in the river long profile are advected upstream at a celerity of $Ce=KA(x)mS(t,x)n^{-1}$ [*Whipple and Tucker*, 1999]. *Whipple and Tucker* [1999] have developed an expression for the time to achieve a new topographic steady state in response to a step change in U, by noting that when U is constant, then so is the rate of vertical migration of knick points. Their expression relies on a more general derivation for the response time that depends on the celerity: , $\tau_{ch} = \int_0^L \frac{dx\prime}{c_e} = \int_0^{L-x_c} \frac{dx\prime}{KA(x\prime)^m S^{n-1}}$,where L is the length of the channel from the outlet to the divide and xc is the distance from the channel head to the divide. Using a similar methodology, *Whipple* [2001] has developed an expression for the time to achieve a new steady state in response to a step change in K.

A different approach for assessing the fluvial response time in the scope of the stream power model relies on analytic solutions of equation (2). Such closed-form solutions have been developed in several studies [e.g., *Luke*, 1972; *Weissel and Seidl*, 1998; *Pritchard et al.*, 2009; *Royden and Perron*, 2013; *Goren et al.*, 2014]. Of these, some have explicitly addressed solutions under the assumption that $n = 1$, i.e., that the incision rate is linear in the slope [e.g., *Royden and Perron*, 2013; *Goren et al.*, 2014]. This assumption ensures that there are no physically unrealized portions of the solutions around migrating knick points [*Royden and Perron*, 2013, and references therein], and therefore, the fluvial response time is well defined.
Goren et al. [2014] have presented a closed form solution to equation (2) for any general history of $U(t)$, a constant K, and under the assumptions that $n = 1$. This solution takes the form of

$$z(t,x) = \int_{t-\tau(x)}^{t} U(t')\, dt', \quad (3)$$

where. $\tau(x) = \int_0^x \frac{dx\prime}{c_e(x\prime)^m} = \int_0^x \frac{dx\prime}{KA(x\prime)^m}$ =Equation (3) means that the elevation, z, of any point, x, along the fluvial channel at time, t, can be expressed if the tectonic uplift rate history, $U(t)$, is known during the time interval between t and $t - \tau(x)$. This time interval, of length $\tau(x)$, can be defined as the response time for any general history of U, although a topographic steady state

cannot be achieved when U varies continuously. Here a similar approach to the fluvial response time is developed, but when both $U(t)$ and $K(t)$ are general functions of time.

Temporal variations in K can arise from changes in the hydraulic conditions of the fluvial system or in the lithological units into which the channel is incising, but they are most commonly related to temporal variations in the climatic conditions. These, in turn, can lead to temporal variations of the water flux [e.g., *Wu et al.*, 2006], the sediment flux [e.g., *Simpson and Castelltort*, 2012] and the rock strength due to climatically controlled chemical weathering [*Murphy et al.*, 2016]. It is important to note that temporal variations in any of these attributes do not necessarily linearly map to temporal variations in K, but commonly, the functional dependency is more complicated. Even for the simplest scenario of variations in precipitation, P, the effect on K is expected to depend on Pm [e.g., *Willett*, 2010; *Ferrier et al.*, 2013]. For simplicity, in the current work, temporal variations of K are generally referred to as temporal variations in the climate without an explicit reference to their specific source or to their exact functional dependency.

Here an analytical solution of equation (2) for general time-dependent boundary conditions of $U(t)$ and $K(t)$ is developed that leads to a definition of the fluvial response time. In this case as well, topographic steady state is not expected, but the response time can be defined as the time interval over which the tectonic rock uplift rate history needs to be known in order to evaluate the topography along the fluvial channel.

2 A Closed Form Analytical Solution of the Linear Stream Power Model

The topography conservation equation for the case of temporally varying U and K and $n = 1$ is expressed as

$$\frac{1}{K(t)}\frac{\partial z}{\partial t} + A(X)^m \frac{\partial z}{\partial x} = \frac{U(t)}{K(t)}. \tag{4}$$

Equation (4) can be written as

$$\frac{dt}{dr}\frac{\partial z}{\partial t} + \frac{dx}{dr}\frac{\partial z}{\partial x} = \frac{dz}{dr} \tag{5}$$

where r is the characteristic parameter, and therefore, the topography, z, varies only as a function of r. In equation (5) the derivatives with respect to r are identified as

$$\frac{dt}{dr} = \frac{1}{K(t)} \text{ subject to } t(r = 0) = S_0 \tag{6}$$

$$\frac{dx}{dr} = A(X)^m \text{ subjected to } x(r = 0) = 0 \tag{7}$$

$$\frac{dz}{dr} = \frac{U(t)}{K(t)} \text{subjected to } z(r = 0) = 0, \tag{8}$$

where s_0 represents the initial conditions. The solution to equation (7) is

$$r(x) = \int_0^x \frac{dx'}{A(X')^m} \tag{9}$$

Here $r(x)$ is found to be $\chi(x)$, the transformation parameter for distance along channel that accounts for the distribution of the upstream drainage area [*Perron and Royden*, 2013]. Originally, for the case of $n = 1$, χ has been defined as, $\chi(x) = \int_0^x \frac{A_0^m dx\prime}{A(x\prime)m'}$where A_0 is a scaling parameter introduced to maintain the dimensionality of χ to [L] [*Perron and Royden*, 2013]. Here r is identified with χ by omitting the scaling parameter, and the dimension of χ becomes [$L^{1-2}m$]. $\chi(x)$ can easily be calculated for any point x along the channel as it only requires knowledge of the drainage area distribution from the outlet to that point and of the value of m, which can be estimated by various techniques [e.g., *Mudd et al.*, 2013; *Goren et al.*, 2014]. The solution to equation (6) is

$$\chi(x) = \int_0^t K(t')dt' - \int_0^{s_0} K(t')\,dt' \tag{10}$$

To simplify equation (10), the following notation is introduced:

$$\Gamma(t) = \int_0^t K(t')dt', \tag{11}$$

Such that the function $\Gamma(t)$ is the integral of $K(t)$ over duration t. Equation (10) can then be written as

$$\chi(\times) = \Gamma(t) - \Gamma(S_0) \tag{12}$$

Next, the inverse function Γ^{-1} is defined, such that Γ^{-1} [Γ (t)] = t, and it is noted that by equation (12): $\Gamma(s_0) = \Gamma(t) - \chi(x)$, and therefore, $s_0 = \Gamma^{-1}[\Gamma(t) - \chi(x)]$. At this stage the solution to equation (8) can be expressed as:

$$z(x,t) = \int_{s_0}^{t} U(t')\mathrm{d}t' = \int_{\Gamma^{-1}[\Gamma(t)-x(x)]}^{t} U(t')dt'. \tag{13}$$

Whose proof is supplied in the supplementary information Equation (13) is a closed form expression for the elevation along the fluvial channel as a function of the fluvial parameters and the tectonic and climatic histories.

Using the definition of the response time as the time interval over which the tectonic history needs to be known in order to find the elevation of a point along the fluvial channel, equation (13) leads to a response time of the form: $t - \Gamma^{-1}[\Gamma(t) - \chi(x)]$. This response time is a function of x, t, and K (t), and thus it varies in both space and time.

3 Predictions for Landscape Evolution

In this section, equation (13) is compared to numerical solutions of equation (4) and is used to make predictions for the evolution of the river profile under various climatic histories. I consider a one dimensional channel, whose drainage area distribution obeys Hack's law [*Hack*, 1957], $A = ka\ (L - x)\ h$, with $h = 2$, ka=2/3, and x is measured from the outlet. The numerical solutions follow the implicit scheme of upstream integration following *Braun and Willett* [2013].

As a first case, consider the simplest scenario where $K(t) = K$ is time independent. Here, $\Gamma(t) = Kt$, and $\Gamma^{-1}(t) = t/K$. Equation (13) can then be written as

$$z(x,t) = \int_{\Gamma^{-1}[\Gamma(t)-\chi(x)]}^{t} U(t')dt' . \int_{\Gamma-1[Kt-\chi(x)]}^{t} U(t')dt' = \int_{t-\frac{\chi(x)}{K}}^{t} U(t')dt', \quad (14)$$

and since $\tau(x) = \chi(x)/K$, the original closed form analytical solution for constant K and variable $U(t)$, equation (3) is recovered. In this case, the response time, $\tau(x) = t - [t - \tau(x)]$, is an inverse function of K, and therefore, higher rates of precipitation, which translate to higher K values, lead to shorter response times. Since the elevation is a function of the response time, higher precipitation rates are expected to result in lower channel relief, as has been observed in nature [e.g., *Ferrier et al.*, 2013; *D'Arcy and Whittaker*, 2014].

Next, consider the case where K increases linearly with time, $K(t) = K_0 t$. Here $\Gamma(t) = K_0 \frac{t^2}{2}$ $\Gamma^{-1}(t) = \sqrt{2t/K_0}$ and. For the complete analytical solution for z, a constant rock uplift rate $U(t) = U_0$ is assumed, and the solution is expressed as

$$z(x,t) = \int_{\Gamma^{-1}[\Gamma(t)-\chi(x)]}^{t} U_0 dt' = U_0 \left[t - \sqrt{t^2 - 2\frac{\chi(\times)}{K_0}} \right]. \quad (15)$$

Figure 1a compares the numerical solution with the analytical solution, equation (15), for this scenario and demonstrates that as time $t \to \infty, z = U_0\left[t - \sqrt{2\chi(x)/K_0}\right] \to$, , i.e., the river profile becomes less steep with time.

As a final example, consider the case where $K(t)$ is a periodic function of time, $K(t) = K_1 + K_0 \cos\left(\frac{2\pi t}{\omega}\right)$ i.e., , where K_0 is the amplitude of the periodic signal, $K_0 < K_1$ to insure positive $K(t)$, and ω is the period. Here. $\Gamma(t) = K_1 t + \frac{K_0 \omega}{2\pi} \sin\left(\frac{2\pi t}{\omega}\right)$.In this case, there is no analytical expression for $\Gamma^{-1}(t)$, but since $\Gamma(t)$ is a monotonically increasing function of t (being an integral of a positive function $K(t)$), and therefore a 1-1 function, the existence of the inverse function is guaranteed. To overcome this limitation, $\Gamma(t)$ is expressed as a discrete mapping, $\Gamma: t \to \Gamma(t)$, and the inverse function Γ^{-1} can be expressed as the inverse mapping $\Gamma^{-1}: \Gamma(t) \to t$. The solution takes the form:

$$z(x,t) = \int_{\Gamma^{-1}[\Gamma(t)-\chi(x)]}^{t} U_0 \mathrm{d}t' = \int_{\Gamma-1\left[K_1 t + \frac{K_0\omega}{2\pi}\sin\left(\frac{2\pi t}{\omega}\right)-\chi(\times)\right]}^{t} U_0 \mathrm{d}t' \quad (16)$$

Figure 1b compares the analytical solution, equation (16), with a discrete mapping for Γ^{-1}, to a numerical solution. The solutions mostly match, and differences across significant slope breaks result from inaccuracy in the numerical solution [*Campforts and Govers*, 2015].

4 Applications

4.1 Landscape Evolution and Numerical Models Validation

The analytic solution, equation (13), can be used to accurately find the evolution of the topography along fluvial channels through time and space, as a function of any general U and K history. Analytic solutions can further be used to validate numerical landscape evolution models and to evaluate their accuracy. *Campforts and Govers* [2015] have shown that both explicit and implicit schemes of advection equations tend to smooth sharp edges (Figure 1b),

and the analytic solution can be used to estimate the degree of smoothing of different numerical schemes.

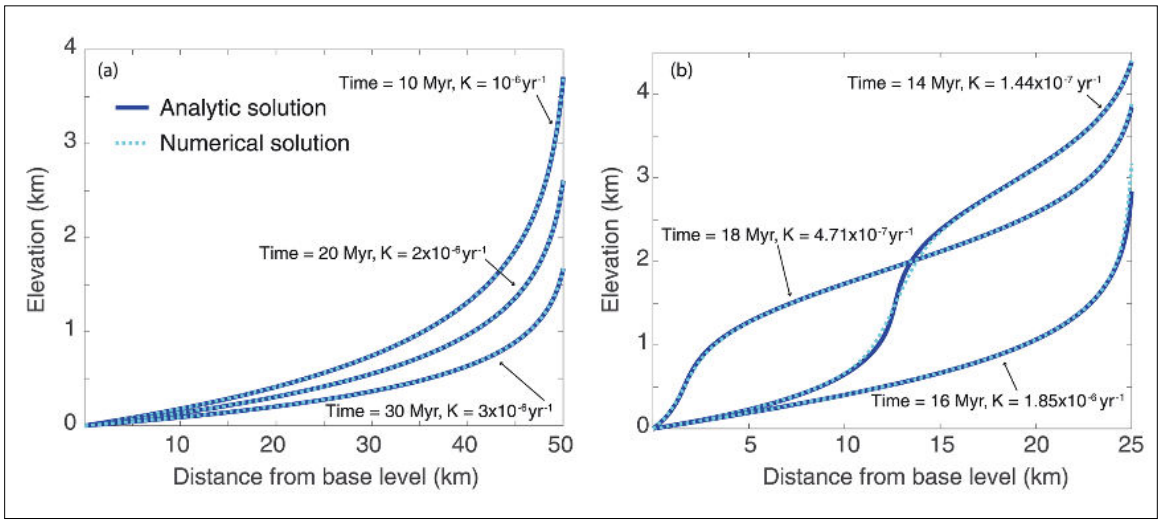

Figure 1.The evolution of river long profile under constant tectonic rock uplift rate, U_0=1 mm/yr and m = 0.5. (a) A linear increase with time of the erosional efficiency K. Solid lines represents the analytic solutions from equation (15). (b) Periodic variability of K with. $K(t) = 10^{-6}\cos\left(\frac{2\pi t}{5\times10^6}\right)$Solid lines represent the analytic solutions of equation (16). In both frames, dashed lines represent the numerical solution of equation (4). Slight mismatch along slope break in Figure 1b arises from numerical diffusion in the numerical scheme.

4.2 Inferring the Climatic History When the Uplift Rate History is Known

Given a river long profile that has developed in response to a known tectonic rock uplift rate history, $U(t)$, and an unknown climatic history, $K(t)$, it is possible to infer $K(t)$ from the elevation data along the channel and the known $U(t)$ via a simple linear inversion. Here the present, when the river long profile is sampled, is taken as $t = 0$. Equation (13) then takes the form:

$$z(\mathrm{x},0) = \int_{\Gamma^{-1}[\Gamma(0)-\chi(\mathrm{x})]}^{0} U(t')dt' = \int_{\Gamma^{-1}[-\chi(\mathrm{x})]}^{0} U(t')dt' \qquad (17)$$

since by definition $\Gamma(0) = 0$. The response time is then

$$\mathrm{ResTime(x)} = -\Gamma^{-1}[-\chi(\mathrm{x})] = \Gamma^{-1}[\chi(\mathrm{x})] \qquad (18)$$

In this framework, the function Γ^{-1} is the mapping Γ^{-1}:$\chi(x)\rightarrow$ResTime(x), and therefore, Γ:ResTime(x)$\rightarrow\chi(x)$. Because by the definition of equation (11), Γ is the integral of $K(t)$, which is the climatic history, $K(t)$ can be found by taking the derivative of Γ, which in this case is the derivative of $\chi(x)$ with respect to ResTime(x), i.e.,

$$K(\mathrm{t} = \mathrm{ResTime(x)}) = \frac{d\chi(\mathrm{x})}{d\mathrm{ResTime(x)}} \qquad 19)$$

For this application, a discrete representation of the fluvial channel is assumed, such that zi and χi=$\chi(xi)$, the elevation and χ value of pixel i, respectively, are known. While the

response time of pixel *i*, ResTime*i*, is still unknown, it can be inferred from the known tectonic rock uplift rate history, $U(t)$. The tectonic rock uplift rate history $U(t)$ can always be discretized over no uniform time intervals such that $U = U_1$ for $0 \le t \le t_1$, $U = U_2$ for $t_1 < t \le t_2$, …, $U = Un$ for $tn_{-1} < t \le tn$. Defining $\Delta t_1 = t_1 - 0$, $\Delta t_2 = t_2 - t_1$, …, $\Delta tn = tn - tn_{-1}$, the elevation zi can be expressed as

$$z_i = \sum_{j=1}^{J} U_j \Delta t_j + U_{J+1} \mathrm{Rem}_i \tag{20}$$

$\mathrm{RemTime}_i$, which is the time interval over which the tectonic rock uplift rate history needs to be known in order to evaluate z_i, is therefore

$$\mathrm{ResTime}_i = \sum_{j=1}^{J} \Delta t_j + \mathrm{Rem}_i \tag{21}$$

Finding ResTime*i* requires an iterative processes of gradually adding terms of the form $Uj\Delta t_j$ for $j = 1, 2$, until z_i is recovered. After ResTime is found, the pixels can be organized in a monotonically increasing order of ResTime, and $K(t)$ can be inferred through equation (19) by differentiating numerically

$$K\left(\mathrm{ResTime}_{j+1/2}\right) = \frac{d\chi_{j+1/2}}{d\mathrm{ResTime}_{j+1/2}} = \frac{\chi_{i+1} - \chi_i}{\mathrm{ResTime}_{j+1} - \mathrm{ResTime}_j} \tag{22}$$

To demonstrate the application of this inversion technique, a river long profile is generated by using the forward model, equation (13), in response to 20 Myr of climatic variability that obeys

$$K(t) = 10^{-6} + 0.9 \times 10^{-6} \sin\left(\frac{2\pi t}{5 \times 10^6}\right), \tag{23}$$

and an uplift rate history of

$$U(t) = \begin{cases} 1 \times 10^{-3} \text{ for } 0 \le t < 2Ma, \\ 3 \times 10^{-3} \text{ for } 2 \le t < 3Ma, \\ 2 \times 10^{-3} \text{ for } 3 \le t < 3.5Ma, \\ 1 \times 10^{-3} \text{ for } 3.5 \le t < 20Ma, \end{cases} \tag{24}$$

The topography, z_i, and the corresponding χ_i are known. It is further assumed that the tectonic history, equation (24), is known. Then by equation (21), the response time of each pixel ResTime*i* is found, and by using equation (22), the climatic history is inferred. Figure 2a compares the imposed and inferred climatic history and shows a good match. Note that the inferred climatic history goes back in time only to the value of max ($\mathrm{ResTime}_j$)

4.3 Inferring the Uplift Rate History When the Climatic History is known

Next, the concept of fluvial response time is used for inferring an unknown rock uplift rate history, when the history of $K(t)$ is known. Here as well, equation (17) is used under the assumption that the present time is represented by $t = 0$. The general inversion methodology follows the one developed in *Goren et al.*[2014] for constant *K*, but an additional, preprocessing step of calculating ResTime*i* for each pixel *i* is needed. This step is trivial, since it is assumed that the function $K(t)$ is known, and therefore, Γ and Γ^{-1} can be calculated and so can ResTime,

through the use of equation (18). From this stage on the *Goren et al.*[2014] methodology can be used as is.

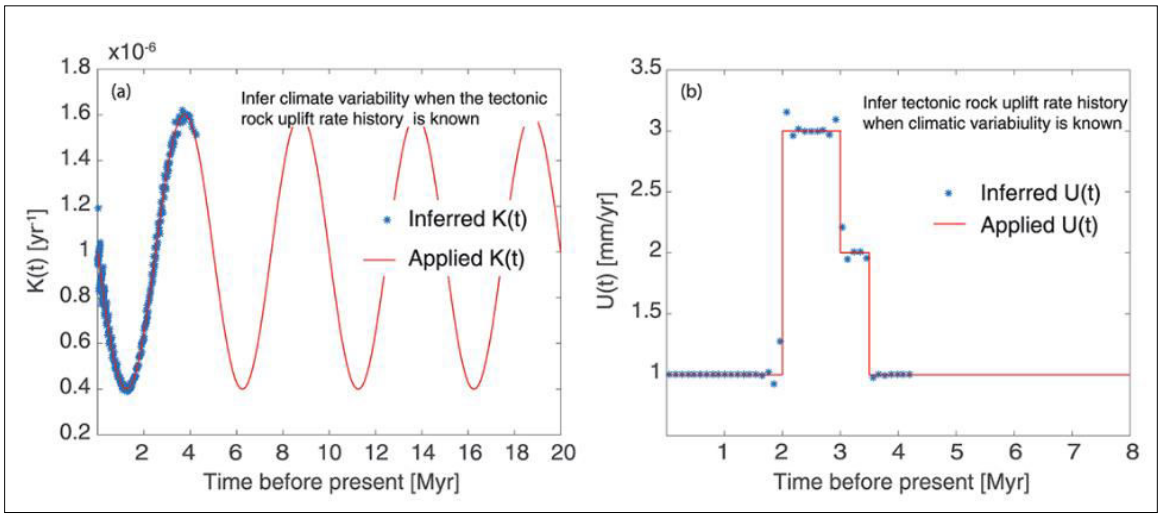

Figure 2 (a) Applied climatic oscillations (solid line) and inferred climatic signal (askterisk) using the inversion scheme presented in section 4.2. The known uplift rate history is given in equation (24). (b) Applied tectonic history (solid line) and inferred history (askterisk) using the inversion scheme from section 4.3. The known climatic variability follows equation (23).

To demonstrate this scheme, the same tectonic and climatic boundary conditions as in the previous problem are used. The topography, z, and the χ values are known and so is the climatic history, equation (23). Figure 2b compares the applied and inferred tectonic rock uplift rate history, showing a good match even along sharp transitions in the tectonic rock uplift rate.

5 Discussions

5.1 Assumptions and Limitations

The analytic derivation, equation (13), relies on several assumptions and simplifications. The first is the linearity between the incision rate and the slope in the stream power model, $n = 1$ in equation (1). The exact value of n has been continuously debated with both supports for $n = 1$ [e.g., *Ferrier et al.*, 2013; *Roberts and White*, 2010] and for $n \neq 1$ [e.g., *Attal et al.*, 2008; *Whittaker and Boulton*, 2012; *Harel et al.*, 2016]. Here linearity is assumed because it uniquely allows developing a simple and closed form solution to equation (2) for any general $U(t)$ and $K(t)$, which then leads to an expression for the fluvial response time. Yet in the supporting information, a scenario with $n = 2$ is explored numerically for the difference between river long profiles with constant and periodic K. Results show qualitatively a similar behavior to that observed for $n = 1$. Second, spatial variations in U [e.g., *Fox et al.*, 2014] and K [e.g., *Roe et al.*, 2002; *Wu et al.*, 2006] are intentionally omitted from the current analysis for simplicity. One possibility for obtaining a solution for the spatially variable case is to divide the channel into segments that experience the same $K(t)$ and $U(t)$ history. Then, the history of $\partial z(t)/\partial t$ of the top most point of one segment, which can be found by time derivation of the forward model, equation (13), can be linearly added to $U(t)$ of its upstream segment, which then can be solved for independently. Finally, the analytical solution requires that the upstream drainage area is temporally invariant, i.e., $A = A(x)$.

An additional limitation of the current analytic approach is that for the general case, the lower bound of the integral solution for z in equation (13) cannot always be written explicitly. As a result, analytical expressions of the slope, $\partial z/\partial x$, of the erosion rate, and of the sediment flux output are not always available. These quantities can still be calculated numerically once the elevation along the channel is accurately resolved by the analytic solution. For this reason, the current study, which focuses on analytic derivations, does not explore the spatial and temporal patterns of erosion rate and sediment flux.

5.2 The Effect of Periodic Climate Change on Landscape Evolution

The analytic solution in equation (13) allows comparing landscape evolution for different climatic scenarios. The comparison between equation (14) that is derived for a constant K and equation (16) that is derived for a periodic K reveals that the solutions differ by the term $\frac{K_0\omega}{2\pi}\sin\left(\frac{2\pi t}{\omega}\right)$ in the parameter of Γ^{-1} at the lower bound of the integral. Γ^{-1} is a continuous function of its parameter, and therefore, when the term $\frac{K_0\omega}{2\pi}\sin\left(\frac{2\pi t}{\omega}\right)$ becomes negligible with respect to χ, the topographic evolution of the periodic K case should converge to that of the constant K case. That is, when, $\frac{K_0\omega}{2\pi} \ll \chi(\mathrm{x})$, the river long profile is not expected to be sensitive to climate periodicity. This means that low-amplitude (K_0) high-frequency ($1/\omega$) climatic oscillations are damped in the river long profile. At the other end-member, when $\frac{K_0\omega}{2\pi} \gtrapprox \chi(\mathrm{x})$, the long profile of rivers that are affected by climate variability should differ from the long profile of constant K rivers. Figure 3a compares between river long profile for constant $K = K_1 = 10^{-6}$ yr^{-1} and for periodic, $K = K_1 + K_0\cos\left(\frac{2\pi t}{\omega}\right)$ with $K_0 = 0.9 \times 10^{-6}$ and different values of ω. The figure shows that as ω decreases the profiles with periodic K gradually become indistinguishable from the profile with constant K. When $\omega > \max(\chi)/K_1$, which sets the response time scale [*Godard et al.*, 2013], the river long profile is in a quasi steady state with respect to the current, instantaneous K value, and no slope breaks are identified. Still, the steepness of the profile (solid thin line in Figure 3a) differs significantly from the steepness of the constant K river (solid thick line in Figure 3a) [e.g., *Allen*, 2008]. When $\omega < \max(\chi)/K_1$, slope breaks appear along the river long profile, preserving older oscillations, but as $\frac{K_0\omega}{2\pi}$ further decreases, these slope breaks become too small to identify (Figure 3a dotted line). This analysis is in line with the numerical work of *Paul et al.* [2014] that has demonstrated in the framework of river long profile inversion, that high-frequency precipitation oscillations do not affect the inferred uplift rates, even when the oscillations are not accounted for.

Figure 3b shows the percent deviation of the topography of the periodic K profiles with respect to the constant K profile. Here again, the case of $\omega > \max(\chi)/K_1$ shows large deviation throughout the profile (Figure 3b solid line). Lower ω cases result in a deviation that decays upstream with increasing χ(Figure 3b dashes and dotted lines). Along the downstream reaches, where $\frac{K_0\omega}{2\pi} \gtrapprox \chi(x)$ large deviation between the profiles is observed, while at the upstream reaches, where $\frac{K_0\omega}{2\pi} \ll \chi(\mathrm{x})$, the deviation is smaller. Supporting information Figure S1 shows that a qualitatively similar behavior of periodic K rivers is observed also when the incision rate depends nonlinearly on the slope, with $n = 2$.

Next, I turn to evaluate the relation between $\frac{K_0\omega}{2\pi}$ and χ for natural fluvial systems. Consider a drainage network that obeys Hack's law. Then

$$\chi\left(x=\int_0^x \frac{dx}{k_a^m(L-x)^{hm}},\right) \tag{25}$$

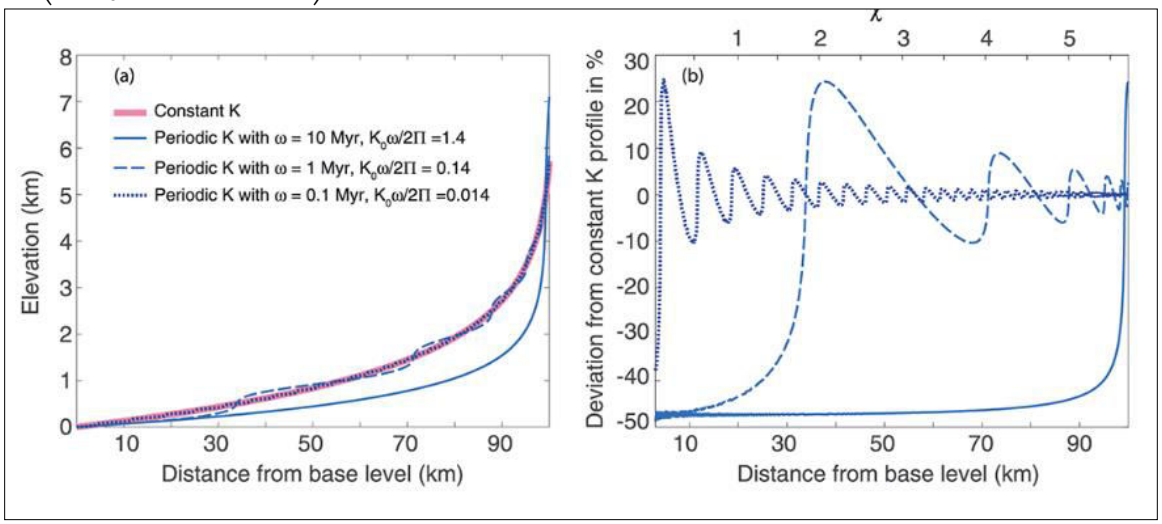

Figure 3. (a) Comparison between constant *K* river profile, solid thick line, and periodic *K* profiles, solid and dashed thin lines, showing that as $\frac{K_0\omega}{2\pi}$ decreases, the periodic *K* profiles approach the constant *K* profile and climatic oscillations and damped. (b) Percent deviation of the periodic *K* profiles from the constant *K* profile, showing that for low χ values (top *x* axis), and close to the outlet, the deviation is larger than at higher χ values and away from the outlet.

where $0 \le x \le L - xc$ ($L - xc$ represents the channel head). The solution of equation (25) is

$$\chi(x) = \frac{1}{k_a^m}\ln\left(\frac{\mathrm{L}}{\mathrm{L}-\mathrm{x}}\right) \text{ for } hm \neq 1. \tag{26}$$

$$= \frac{1}{k_a^m(1-\mathrm{hm})}\left[L^{1-\mathrm{hm}} - (L-\mathrm{x})^{1-\mathrm{hm}}\right] \text{ for } hm \neq 1. \tag{27}$$

Assuming ka=2/3, h = 2, L = 50 km, and xc=1 km. Then, for m = 0.5, $\chi(L/2)$ = 0.85 and $\chi(L - xc)$ = 4.79, while for m = 0.4, $\chi(L/2)$ = 6.63 and .$\chi(L - \mathrm{x}_c)$ This calculation shows that for the parameters used here, the top half of the fluvial channel is characterized by . $\chi = \mathcal{O}(1) - \mathcal{O}(10)$The period of natural climatic oscillations related to Milankovitch cycles are of the order of 10^4–10^5 yr. Considering K_0 to be of the order of the erosional efficiency, i.e., 10^{-7}–10^{-5} yr^{-1} [*Stock and Montgomery*, 1999; *Snyder et al.*, 2000] (for m = 0.5), then$1.6 \times 10^{-4} < \frac{K_0\omega}{2\pi} < 0.16$. It is therefore clear that in the majority of the cases, the condition$\frac{K_0\omega}{2\pi} \ll \chi(x)$ is met, and accordingly, Milankovitch climatic oscillations are not expected to leave a significant fingerprint on the higher reaches of river long profiles.

The above analysis has two implications for the possibility of inferring climatic and tectonic signals from river long profiles. First, in cases where $\frac{K_0\omega}{2\pi}$ can be shown to be $\ll\chi$, climatic oscillations are not expected to significantly affect the river long profile, and a constant *K* value can be assumed when recovering the tectonic signal with either forward [e.g., *Whittaker et al.*, 2008] or inverse [e.g., *Paul et al.*, 2014; *Goren et al.*, 2014] modeling. Indeed, using the algorithm presented in section 4.3, C. Petit et al. (personal communication, 2016) have demonstrated that inversion of the Tinee river tributaries for its main trunk incision

history [*Petit et al.*, 2016] results in similar inferred histories when using constant K or periodic $K$with a period of $\sim 10^5$ yr and $K_0 \approx 0.5 \times 10^{-5}$ $m^{1-2}m$/yr. Second, since the lower reaches, close to the outlet, are always characterized by lower χ values, for these reaches $\frac{K_0 \omega}{2\pi} > \chi(x)$ and the climatic signature is expected to affect the river long profile. Albeit, due to the expected low elevation and slope of these reaches, such a signature is harder to identify.

The above outcomes should be considered with some caution when additional effects that may influence the river long profile during Milankovitch climate oscillations are significant. Such effects include changes in the erosional mechanism from fluvial to glacial [*Valla et al.*, 2010], base level changes related to climatic oscillations [*Lambeck and Bard*, 2000] and grain size [*Peizhen et al.*, 2001; *D'Arcy*, 2015] and sediment flux [*Simpson and Castelltort*, 2012] oscillations that may nonlinearly affect K. Furthermore, the lack of topographic signature of high-frequency climatic oscillations does not imply that the commulative erosion and sediment output from detachment-limited rivers are insensitive to these oscillations. On the contrary, *Godard et al.* [2013] have demonstrated numerically that the time series of sediment flux of rivers that obey the stream power model follows the imposed high-frequency climatic oscillations.

6 Conclusions

This work solves analytically the linear stream power fluvial incision model for any general tectonic, $U(t)$, and climatic, $K(t)$, histories. From the solution, a general definition of the fluvial response time arises, which is valid even when topographic steady state cannot be achieved. According to this definition, the response time is the time over which the tectonic rock uplift rate history needs to be known in order to constrain the elevation of a point, x, along a fluvial channel at a given time, t. This response time is a function of x, t, and $K(t)$. The new definition of the response time allows developing linear inverse models that use the long profile of rivers to infer the tectonic history when the climate history is known, and to infer the climate history when the tectonic history is known. Investigation of this response time when $K(t)$ is periodic reveals that high-frequency low-amplitude oscillations, such as Milankovitch cycles, are topographically damped and are therefore not expected to leave their mark along the higher reaches of river long profiles.

References

Allen, P. A. (2008), Time scales of tectonic landscapes and their sediment routing systems, *Geol. Soc. London Spec. Publ., 296(1),* 7-28, doi:10.1144/SP296.2.

Amos, C. B., and D. W. Burbank (2007), Channel width response to differential uplift, *J. Geophys. Res., 112,* F02010, doi:10.1029/2006JF000672.

Armitage, J. J., T. D.Jones, R. A. Duller, A. C. Whittaker, and P. A. Allen (2013), Temporal buffering of climate-driven sediment flux cycles by transient catchment response, *Earth Planet. Sci. Lett., 369-370,* 200-210, doi:10.1016/j.epsl.2013.03.020.

Attal, M., G. E. Tucker, A. C. Whittaker, P. A. Cowie, and G. P. Roberts (2008), Modeling fluvial incision and transient landscape evolution: Influence of dynamic channel adjustment, *J. Geophys. Res., 113,* F03 013, doi:10.1029/2007JF000893.

Braun, J., and S. D. Willett (2013), A very efficient O(n), implicit and parallel method to solve the stream power equation governing fluvialincision and landscape evolution, *Geomorphology, 180-181,*170-179, doi:10.1016/j.geomorph.2012.10.008.

Campforts, B., and G. Govers (2015), Keeping the edge: A numerical method that avoids knickpoint smearing when solving the stream power law, *J. Geophys. Res. Earth Surf.,* 120,1189-1205, doi:10. 1002/2014JF003376.

D'Arcy, M. (2015), Glacial-interglacial climate changes recorded by debris flow grain size, Eastern Sierra

Nevada, California, AbstractEP33B-1077 presented at 2015 Fall Meeting, AGU, San Francisco, Calif., 14-18

Dec. D'Arcy, M., and A. C. Whittaker (2014), Geomorphic constraints on landscape sensitivity to climate in tectonically active areas,*Geomorphology, 204,*366-381, doi:10.1016/j.geomorph.2013.08.019.

DiBiase, R. A., and K. X. Whipple (2011), The influence of erosion thresholds and runoff variability on the relationships among topography, climate, and erosion rate, *J. Geophys. Res., 116,* F04036, doi:10.1029/2011JF002095.

Ferrier, K. L., K. L. Huppert, and J. T. Perron (2013), Climatic control of bedrock river incision, *Nature,* 496(7444), 206-209,doi:10.1038/nature11982.

Finnegan, N. J., G. Roe, D. R. Montgomery, and B. Hallet (2005), Controls on the channel width of rivers: Implications for modeling fluvialincision of bedrock, *Geology,* 33(3), 229-232, doi:10.1130 /G21171.1.

Fox, M., L. Goren, D. A. May, and S. D. Willett (2014), Inversion of fluvial channels for paleorock uplift rates in Taiwan, *J. Geophys. Res. Earth Surf.,* 119,1853-1875, doi:10.1002/2014JF003196.

Gasparini, N. M., and M. T. Brandon (2011), A generalized power law approximation for fluvial incision of bedrock channels, *J. Geophys. Res., 116,* F02020, doi:10.1029/2009JF001655.

Gasparini, N. M., K. X. Whipple, and R. L. Bras (2007), Predictions of steady state and transient landscape morphology using sediment-flux-dependent river incision models, *J. Geophys. Res., 112,* F03S09, doi: 10.10 2 9 /2006JF000567.

Godard, V., G. E. Tucker, G. Burch Fisher, D. W. Burbank, and B. Bookhagen (2013), Frequency Depen dent landscape response to climaticforcing, *Geophys. Res. Lett., 40,*859-863, doi:10.1002 /grl.50253.

Goren, L., M. Fox, and S. D. Willett (2014), Tectonics from fluvial topography using formal linear inversion: Theory and applications to the Inyo Mountains, California, *J. Geophys. Res. Earth Surf., 119,*1651-1681, doi:10.1002/2014JF003079.

Hack, J. T. (1957), Studies of Longitudinal stream profiles in Virginia and Maryland, *USGS Prof. Pap.* 294-6,45-97, U.S. Govt.Print.Off.,Washington, D. C.

Harel, M.-A., S. Mudd, and M. Attal (2016), Global analysis ofthe stream power law parameters based on worldwide 10Be denudation rates,*Geomorphology, 268,*184-196, doi:10.1016/j.geomorph. 201 6.05 .035.

Howard, A. D. (1994), A detachment limited model of drainage-basin evolution, *Water Resour. Res., '* 30(7), 2261 -2285,doi:10.1029/94WR00757.

Howard, A. D., and G. Kerby (1983), Channel changes in badlands, *Geol. Soc. Am. Bull.,* 94(6), 739-752.

Lague, D. (2014), The stream power river incision model: Evidence, theory and beyond, *Earth Surf. Processes Landforms, 39*(1), 38-61,doi:10.1002/esp.3462.

Lague, D., N. Hovius, and P. Davy (2005), Discharge, discharge variability, and the bedrock channel profile, *J. Geophys. Res., 110,* F04006,doi:10.1029/2004JF000259.

Lamb, M. P., W. E. Dietrich, and L. S. Sklar (2008), A model for fluvial bedrock incision by impacting suspended and bed load sediment, *J. Geophys. Res., 113,* F03025, doi:10.1029/2007JF000915.

Lambeck, K., and E. Bard (2000), Sea-level change along the French Mediterranean coast for the past 30000 years, *Earth Planet. Sci. Lett.,175(3* -4), 203-222, doi:10.1016/S0012-821X(99)00289-7.

Luke, J. C. (1972), Mathematical models for landform evolution, *J. Geophys. Res.,* 77(14), 2460-2464, doi:10.1029/JB077i014p02460.

Mudd, S. M. (2016), Detection of transience in eroding landscapes, *Earth Surf. Processes Landforms,* doi:10.1002/esp.3923.

Mudd, S. M., M. Attal, D. T. Milodowski, S. W. Grieve, and D. A. Valters (2013), A statistical framework to quantify spatial variation in channel gradients using the integral method of channel profile analysis, *J. Geophys. Res Earth Surf., 119,*138-152, doi:10.1002/2013JF002981.

Murphy, B. P., J. P. L.Johnson, N. M. Gasparini, and L. S. Sklar (2016), Chemical weathering as a mechanism for the climatic control of bedrock river incision, *Nature,* 532(7598), 223-227, doi:10.1038/ nature17449.

Parker, G. (1991), Selective sorting and abrasion of river gravel. I: Theory, *J. Hydraul. Eng.,* 117(2), 131-149.

Paul, J. D., G. G. Roberts, and N. White (2014), The African landscape through space and time, *Tectonics, 33,* 898-935,doi:10.1002/2013TC003479.

Peizhen, Z., P. Molnar, and W. R. Downs (2001), Increased sedimentation rates and grain sizes 2-4 Myr

ago due to the influence of climatechange on erosion rates, *Nature,* 410(6831), 891 -897, doi:10.1038 /35073504.
Perron, J. T., and L. Royden (2013), An integral approach to bedrock river profile analysis, *Earth Surf. Processes Landforms, 38,* 570-576,doi:10.1002/esp.3302.
Petit, C., D. Cassol, Y. Rolland, and M. Saillard (2016), Late Quaternary incision rates in the southern French Alps from river longitudinal profiles inversion: Climatic forcing and internal adjustments, Geophysical Research Abstracts EGU2016-8134 presented at 2016 EGU General Assembly, Vienna, 17-22 Apr.
Pritchard, D., G. G. Roberts, N. J. White, and C. N. Richardson (2009), Uplift histories from river profiles, *Geophys. Res. Lett., 36,* L24301,doi:10.1029/2009GL040928.
Roberts, G. G., and N. White (2010), Estimating uplift rate histories from river profiles using African ‘ examples, *J. Geophys. Res., 115,* B02406,doi:10.1029/2009JB006692.
Roe, G. H., D. R. Montgomery, and B. Hallet (2002), Effects of orographic precipitation variations on the concavity of steady-state river profiles, *Geology,* 30(2), 143-146, doi:10.1130/0091-7613(2002) 030 <0143: EOOPVO>2.0.CO;2.
Romans, B. W., S. Castelltort, J. A. Covault, A. Fildani, and J. Walsh (2016), Environmental signal propag ation in sedimentary systems acrosstimescales, *Earth Sci. Rev., 153,* 7 - 29, doi:10.1016/j .earsci rev. 2015.07.012.
Royden, L., and J. T. Perron (2013), Solutions ofthe stream power equation and application to the evolution of river longitudinal profiles,*J. Geophys. Res. Earth Surf., 118,*497-518, doi:10.1002/jgrf.20031.
Simpson, G., and S. Castelltort (2012), Model shows that rivers transmit high-frequency climate cycles to the sedimentary record, *Geology,*40(12), 1131-1134, doi:10.1130/G33451.1.
Sklar, L., and W. E. Dietrich (1998), River longitudinal profiles and bedrock incision models: Stream power and the influence of sedimentsupply, in *Rivers Over Rock: Fluvial Processes in Bedrock Channels, Geophys. Monogr. Ser.,* vol. 107, edited by K. J. Tinkler and E. E. Wohl,pp. 237-260, AGU, Washington, D. C.
Snyder, N. P., K. X. Whipple, G. E.Tucker, and D.J. Merritts (2000), Landscape response to tectonic forcing: Digital elevation model analysis of stream profiles in the Mendocino triple junction region, northern California, *Geol. Soc. Am. Bull.,* 112(8), 1250-1263.
Snyder, N. P., K. X. Whipple, G. E.Tucker, and D.J. Merritts (2003), Importance of a stochastic Distribu tion of floods and erosion thresholds in the bedrock river incision problem, *J. Geophys. Res.,* 108(B2), 2117, doi:10.1029/2001JB001655.
Stock, J. D., and D. R. Montgomery (1999), Geologic constraints on bedrock river incision using the stream power law, *J. Geophys. Res.,*104(B3), 4983 -4993, doi:10.1029/98JB02139. ‘
Turowski, J. M., and D. Rickenmann (2009), Tools and cover effects in bedload transport observations in the Pitzbach, Austria, *Earth Surf. Processes Landforms,* 34(1), 26-37, doi:10.1002/esp.1686.
Turowski, J. M., D. Lague, A. Crave, and N. Hovius (2006), Experimental channel response to tectonic uplift, *J. Geophys. Res., 111,* F03008, doi:10. 1029 /2005JF000306.
Valla, P. G., P. A. van der Beek, and D. Lague (2010), Fluvial incision into bedrock: Insights from morphometric analysis and numerical modeling of gorges incising glacial hanging valleys (Western Alps, France), *J. Geophys. Res., 115,* F02010, doi:10.1029/2008JF001079.
Weissel, J. K., and M. A. Seidl (1998), Inland propagation of erosional escarpments and river profile evolution across the southeast Australian passive continental margin, in *Rivers Over Rock: Fluvial Processes in Bedrock Channels, Geophys. Monogr. Ser.,* vol. 107, edited by J. Tinkler and E. E. Wohl, pp. 189-206, AGU, Washington, D. C.
Whipple, K. X. (2001), Fluvial landscape response time: How plausible is steady-state denudation?, *Am.J.Sci.,* 301(4-5), 313-325,doi:10.2475/ajs.301.4-5.313.
Whipple, K. X., and G. E. Tucker (1999), Dynamics ofthe stream-power river incision model: Implications for height limits of mountainranges, landscape response timescales, and research needs, *J. Geophys. Res.,* 104(B8), 17,661-17,674, doi:10.1029/1999JB900120.
Whittaker, A. C., and S. J. Boulton (2012), Tectonic and climatic controls on knickpoint retreat rates and landscape response times, *J. Geophys. Res., 117,* F02024, doi:10.1029/2011JF002157.
Whittaker, A. C., M. Attal, P. A. Cowie, G. E. Tucker, and G. Roberts (2008), Decoding temporal and spatial patterns of fault uplift usingtransient river long profiles, *Geomorphology,* 100(3-4), 506-526, doi:10.1016/j.geomorph.2008.01.018.
Wilcock, P. R. (1998), Two-fraction model of initial sediment motion in gravel-bed rivers, *Science,*

280(5362), 410-412,doi:10.1126/science.280.5362.410.